Photochemical Phosphorus-Enabled Scaffold Remodeling of Carboxylic Acids

Authors: Qiupeng Peng[1], Meemie U. Hwang[1], Ángel Rentería-Gómez[2], Poulami Mukherjee[2], Ryan M. Young[1,3], Yunfan Qiu[1,3], Michael R. Wasielewski[1,3], Osvaldo Gutierrez[2], and Karl A. Scheidt*[1]

Affiliations:

[1]Department of Chemistry, Northwestern University, 2145 Sheridan Road, Evanston, IL 60208, USA.
[2]Department of Chemistry, Texas A&M University, College Station, Texas 77843, USA.
[3]Institute for Sustainability and Energy at Northwestern, Northwestern University, Evanston, Illinois 60208, United States.

*Corresponding author. KAS: scheidt@northwestern.edu

Abstract:

The excitation of carbonyl compounds by light to generate radical intermediates is a distinctive mode of molecular activation. These processes play important roles in organic synthesis, especially for the challenging formation of carbon-carbon bonds that conventional two-electron chemical processes are unable to achieve. This approach has historically been restricted to ketones and aldehydes, and carboxylic acids have been overlooked due to high energy requirements and their low quantum efficiency. The development of a robust and general method for the direct excitation of carboxylic acid derivatives holds significant promise for advancing the field of chemistry. A successful activation method strategy necessitates a bathochromic shift in the absorbance profile, an increase in triplet diradical lifetime, and ease of further functionalization. We present a phosphorus-based strategy through a single-flask transformation of carboxylic acids into acyl phosphonates that access synthetically useful triplet diradicals under visible light or near-ultraviolet irradiation. The use of phosphorus circumvents unproductive Norrish type I processes, promoting selectivity that enables new hydrogen atom transfer (HAT) logic and facilitates diverse reactivity. Employing this strategy promotes the efficient scaffold remodeling of carboxylic acids through various annulation, contraction, and expansion manifolds. This expansion of HAT logic enabled by easily accessed acyl phosphonates represents significant potential for pharmaceuticals, materials science, and environmental applications.

Photochemical processes that harness light to promote new bond-forming processes are inherently sustainable and provide exciting opportunities to leverage excited state/radical behavior in contrast to traditional reactivity[1-5]. Since Norrish[6] first reported the photoexcitation of ketones in 1937 and Yang's[7] observation in 1958 that excited ketones undergo rapid fragmentation, the photochemistry of carbonyl-containing molecules has progressed significantly[8]. Various bond-forming processes involving formal [2+2] cycloadditions[9,10] such as the Paterno-Büchi and DeMayo reactions have been utilized in complex synthesis[11-13]. However, this established photoexcitation strategy encounters persistent challenges, including controlling α-cleavage that promotes the homolysis of carbon-carbon bonds leading to the formation of two radical species (Norrish type I) as well as hydrogen atom transfer (HAT) processes, resulting in unproductive enol and alkene formation[14] (Norrish type II, Fig.1a). Notably, in comparison to the well-explored photochemistry of ketones[15], carboxylic acids and their derivatives have received comparatively far less attention due to their absorption in far-ultraviolet light and low quantum efficiency[16] (Fig.1b). Innovative strategies involving related energy transfer for the excitation of carbon-carbon double bonds in unsaturated systems leading to triplet diradicals[17-19] has emerged as one way to modulate excited carbonyl processes. However, the energy transfer process for the carbonyl group of carboxylic acid derivatives requires significantly higher energy which impedes this pathway[20,21]. Consequently, there is a captivating opportunity for a strategy to address this challenge with acids, thus potentially opening new activation modes and broadening the utilization of carboxylic acids[22,23] and their derivatives[24] in photochemical processes.

The main design challenge to engage carboxylic acids directly with light to promote photoexcited reactivity is the lack of reactivity with this functional group. To address this issue, an ideal method for carboxylic acid engagement via modification should involve direct transformation from free carboxylic acids without purification, coupled with a bathochromic shift in the absorbance profile. This shift would enable direct photoexcitation under visible light or near-ultraviolet light without the need for a sensitizer. The activated intermediate will subsequently generate the singlet diradical before intersystem crossing to access the triplet diradical[25] which would have a significantly increased lifetime compared to the triplet state of ketones. If successful, this approach would enable control over diradical reactivity, diminish or even eliminate the Norrish type I reaction, and access a new HAT logic encompassing 1,5-HAT, 1,6-HAT, and 1,7-HAT processes while promoting the diradical with broad reactivity (Fig.1c).

The proposed approach utilizes a phosphorus promoter as an effective choice to realize this process while also establishing a functional handle for subsequent transformations[26-29]. Our phosphorus promoter design enables diverse scaffold remodeling, encompassing annulation, contraction, and expansion. Scaffold remodeling[30,31], sometimes referred to as skeletal editing, harbors significant potential for augmenting molecular diversity and complexity, thereby propelling advancements in pharmaceuticals, materials science, and environmental technologies. To illustrate, a variety of carboxylic acids were selected as starting materials and sequentially activated by oxalyl chloride and trimethyl phosphite to generate acyl phosphonates[32]. Subsequently, photoexcitation to the singlet diradical state followed by intersystem crossing gives access to the triplet excited state. For β/γ-amino acids, the generated triplet diradical undergoes a selective [1,6]/[1,7]-HAT process to form [1,5]/[1,6]-diradical intermediates which in turn leads to intramolecular radical-radical coupling and cyclized product formation. In the case of α-proline derivatives, a preference for the [1,5]-HAT process results in a [1,4]-diradical intermediate. This intermediate undergoes homolytic carbon-nitrogen bond cleavage, generating imine- and enol-containing species before O-nucleophilic addition yields the expanded ring product. For pipecolic acids, the same strategy is

utilized to generate imine- and enol-containing intermediates which form the final ring contraction product via Mannich reaction due to preference towards the more stable five-membered ring rather than unfavored seven-membered ring. (Fig. 2a).

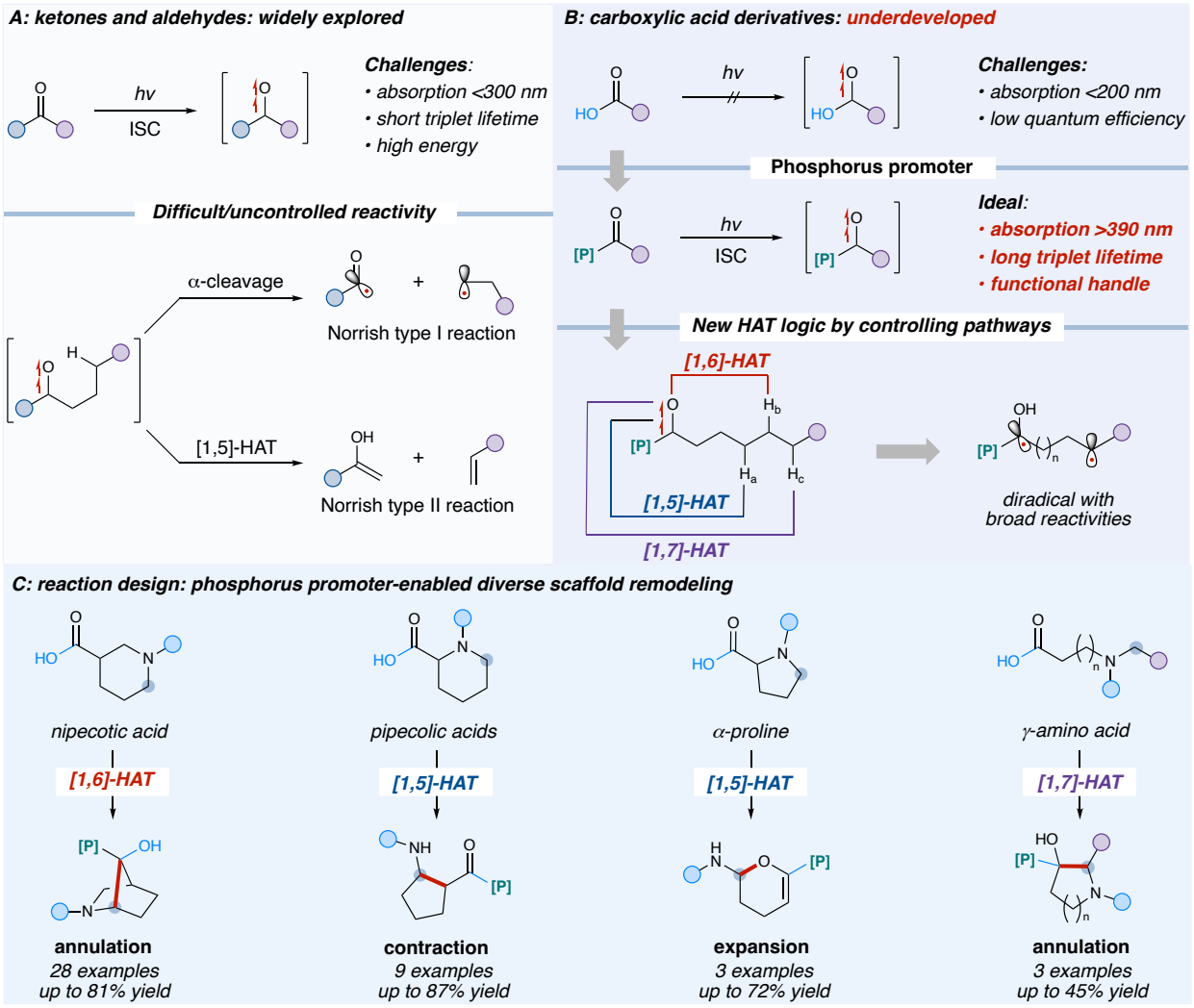

Fig. 1. Visible light-induced carboxylic acid scaffold remodeling via chromophore strategy a) Photoexcitation of ketones and aldehydes. b) The challenges and opportunities for photoexcitation of carboxylic acids. c) The phosphorus-promoter enabled diverse scaffold remodeling carboxylic acids.

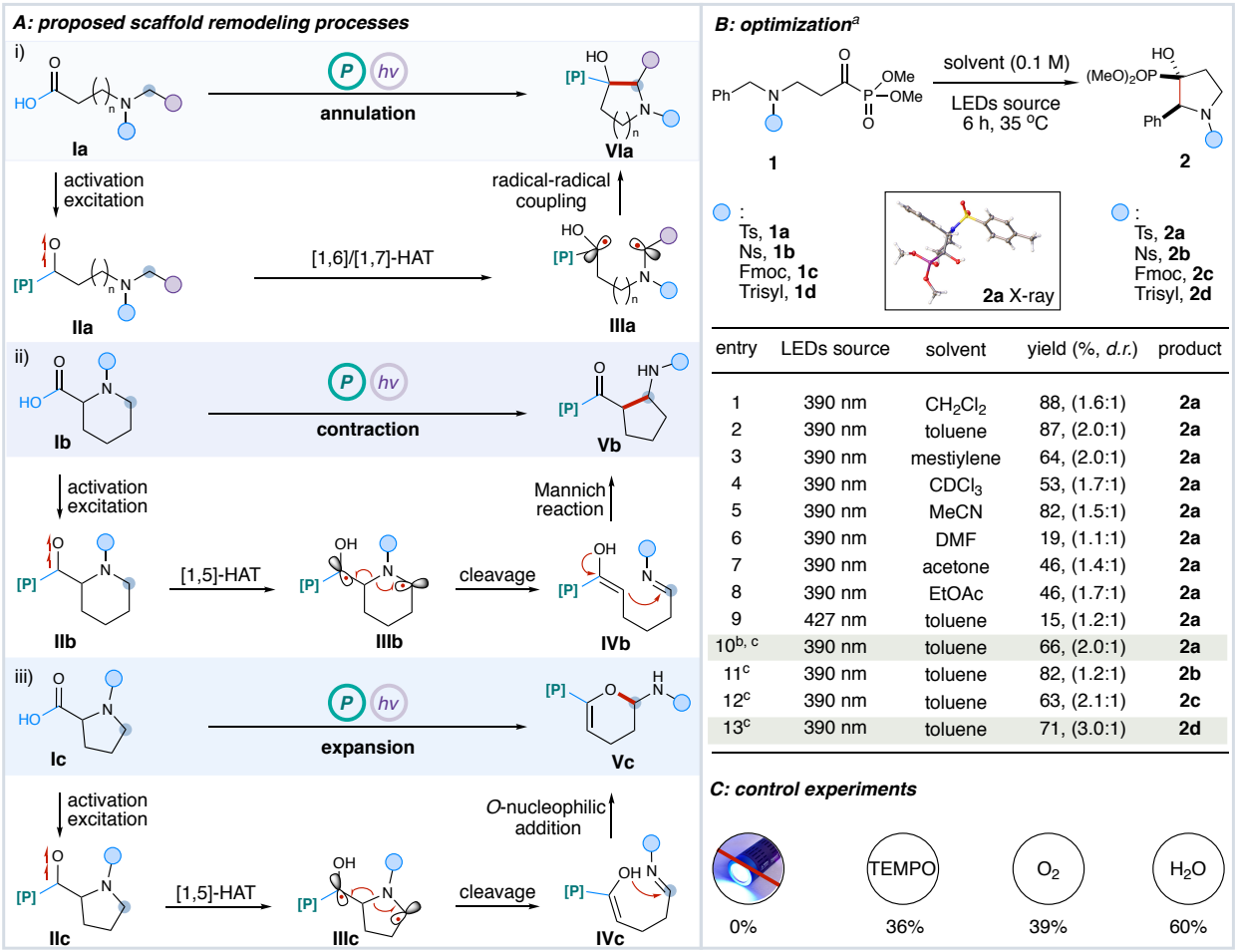

entry	LEDs source	solvent	yield (%, *d.r.*)	product
1	390 nm	CH_2Cl_2	88, (1.6:1)	**2a**
2	390 nm	toluene	87, (2.0:1)	**2a**
3	390 nm	mestiylene	64, (2.0:1)	**2a**
4	390 nm	$CDCl_3$	53, (1.7:1)	**2a**
5	390 nm	MeCN	82, (1.5:1)	**2a**
6	390 nm	DMF	19, (1.1:1)	**2a**
7	390 nm	acetone	46, (1.4:1)	**2a**
8	390 nm	EtOAc	46, (1.7:1)	**2a**
9	427 nm	toluene	15, (1.2:1)	**2a**
10[b, c]	390 nm	toluene	66, (2.0:1)	**2a**
11[c]	390 nm	toluene	82, (1.2:1)	**2b**
12[c]	390 nm	toluene	63, (2.1:1)	**2c**
13[c]	390 nm	toluene	71, (3.0:1)	**2d**

Fig. 2. a) The scaffold remodeling mechanisms for β/γ-amino acids, α-prolines, and pipecolic acids. b) β-amino acid scaffold remodeling reaction optimization table. [a]0.10 mmol scale, acyl phosphonate as starting material, yield determined by ^{1}H NMR using 1,3,5-trimethoxybenzene as internal standard, diastereomeric ratios determined by ^{1}H NMR analysis of unpurified reaction mixtures, major diastereomer was assigned by X-ray crystallography; [b]10.0 mmol scale, yield after recrystallization from toluene and dichloromethane (20:1, v/v); [c]Carboxylic acids as starting materials. c) Control experiments: 0.10 mmol, acyl phosphonate **1d** as starting material; no irradiation; 2.0 equivalents of TEMPO; under oxygen atmosphere; 10.0 equivalents of water were added

Reaction development

The optimization process commenced with acylphosphonate **1a** as the model substrate (Fig. 2b). The utilization of non-polar solvents such as dichloromethane, toluene, and chlorobenzene facilitated the smooth production of the desired product with high yields and moderate diastereoselectivity (Fig. 2b, entries 1 - 4). Conversely, more polar solvents, e.g., DMF, acetone, and ethyl acetate, yielded only moderate conversion with a correspondingly lower yield (Fig. 2b, entries 5 - 8). By transitioning to a light source emitting at 427 nm blue LEDs (Fig. 2b, entry 9), a noteworthy deceleration in the reaction rate was observed. In the subsequent refinement of the reaction conditions, toluene was selected as the solvent, demonstrating its efficacy in the single-

flask version for the synthesis of carboxylic acid-derived products. Notably, this protocol exhibited robustness at larger scales, as evidenced by the successful generation of the desired product on a 2.4 g scale (66% yield over three steps) without the need for chromatographic purification (Fig. 2b, entry 10). The transposition of **2a** to 3-pyrrolidone was exemplified upon treatment with LiHMDS, affording a yield of 79% (see the Supporting Information for additional details). Alteration of the protecting group (Fig. 2b, entries 11 - 13) between Ts (toluenesulfonyl), Ns (naphthalene-2-sulfonyl), Fmoc (fluorenylmethoxycarbonyl), and to the bulkier trisyl (2,4,6-triisopropylbenzenesulfonyl) group (71% yield over three steps, 89% average yield for each step) resulted in a subtle enhancement in diastereoselectivity. In addition, a series of control experiments were conducted to confirm the indispensable role of light in the generation of diradical species (Fig. 2c). The introduction of radical scavengers such as TEMPO was found to markedly diminish the overall yield, supporting the operation of a single electron process. In addition, the presence of a triplet quencher, oxygen, resulted in a significantly decreased yield. In a surprising outcome, the addition of 10.0 equivalents of water did not impede the formation of the desired product, yielding a satisfactory outcome.

Fig. 3. Substrate scope for β/γ–amino acid annulation via [1,6]/[1,7]-HAT process[a]

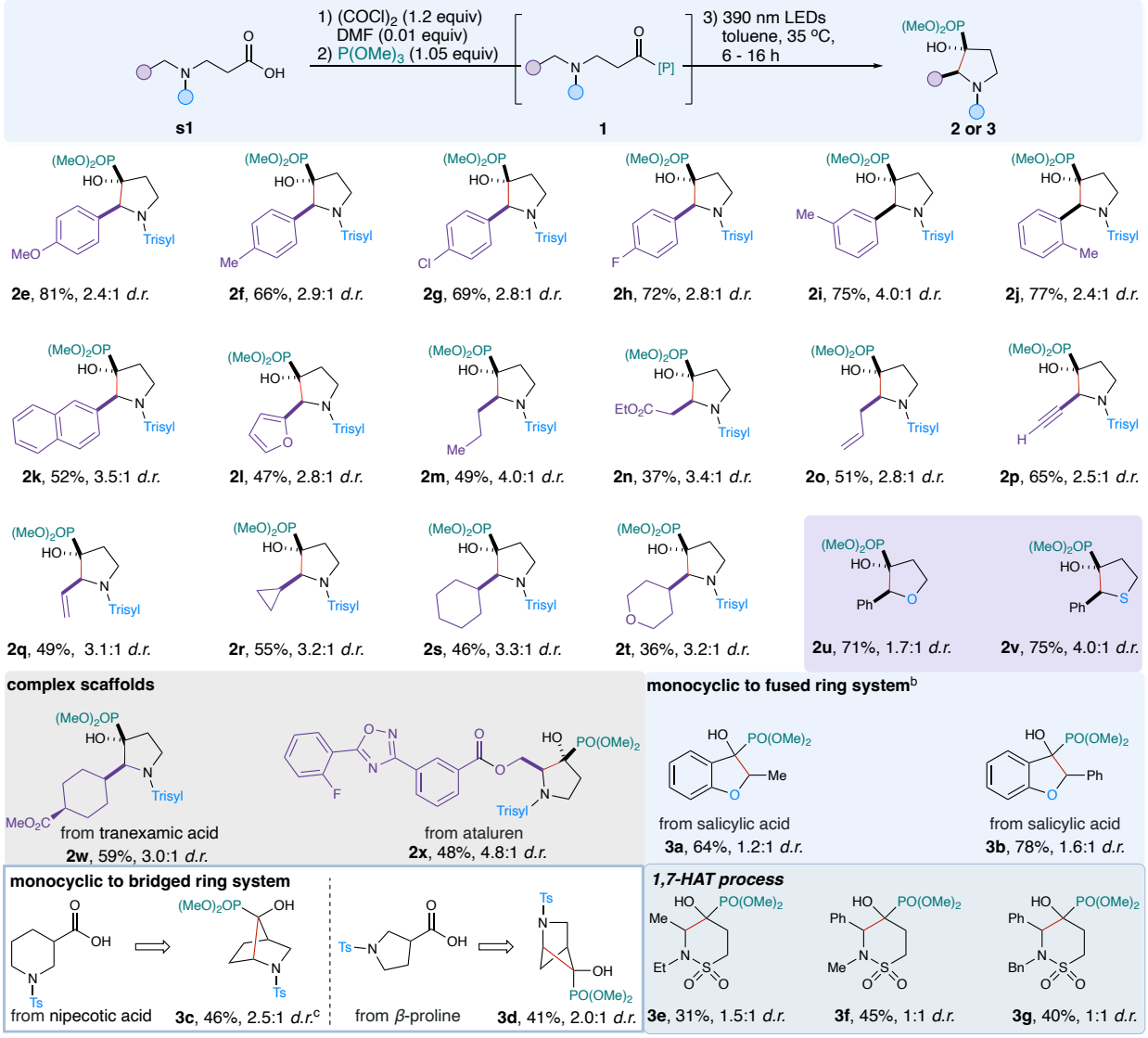

[a]0.20 mmol scale, carboxylic acid as starting material, isolated yield reported, diastereomeric ratios determined by ^{1}H NMR spectroscopic analysis of unpurified reaction mixtures. [b]456 nm LEDs were used. [c]MeCN was solvent.

With the optimized conditions established, an extended exploration of substrate scope was commenced (Fig. 3). When employing a variety of phenyl ring substitutions encompassing both electron-withdrawing and electron-donating groups, our methodology consistently yielded the desired products with commendable yields (**2e** – **2j**). Naphthalene and furan-substituted β-amino acids also furnished the corresponding products with acceptable yields (**2k**, **2l**). The reactivity of linear alkyl-substituted β-amino acid starting materials was investigated under identical conditions, resulting in their smooth conversion to pyrrolidines with modest yields (**2m** - **2o**). Furthermore, investigations into the propargyl (**2p**) and allylic (**2q**) C-H bond-containing substrates revealed their susceptibility to a 1,6-HAT process, yielding the targeted products. Notably, the examination of cyclopropane-substituted starting materials yielded exclusively the normal annulation product (**2r**), with no detection of ring-opened products. Encouragingly, the presence of cyclohexane and tetrahydro-2*H*-pyran moieties did not impede reactivity (**2s** – **2t**). Moreover, the transformations of β-hydroxy acid and β-thio acid derivatives yielded tetrahydrofuran (**2u**) and tetrahydrothiophene (**2v**) scaffolds, respectively. Expanding the applications of this strategy, tranexamic acid and ataluren derivatives were obtained with modest yields (**2w** - **2x**). Salicylic acid derivatives were effectively converted into fused rings (**3a**, **3b**). Notably, cyclic β-amino acids, e.g., nipecotic acids (**3c**) and β-proline (**3d**), demonstrated the formation of more intricate [2,2,1] or [2,1,1] bridged rings under the optimized conditions, showcasing the utility of the methodology in synthesizing structurally demanding yet valuable compounds[33,34]. A more challenging 1,7-HAT process was also successfully realized (**3e** - **3g**), albeit with reduced yields, presenting an intriguing avenue for further investigation, particularly in medicinal applications.

Fig. 4. Substrate scope for cyclo-α–amino acid ring contraction/expansion via [1,5]-HAT process.

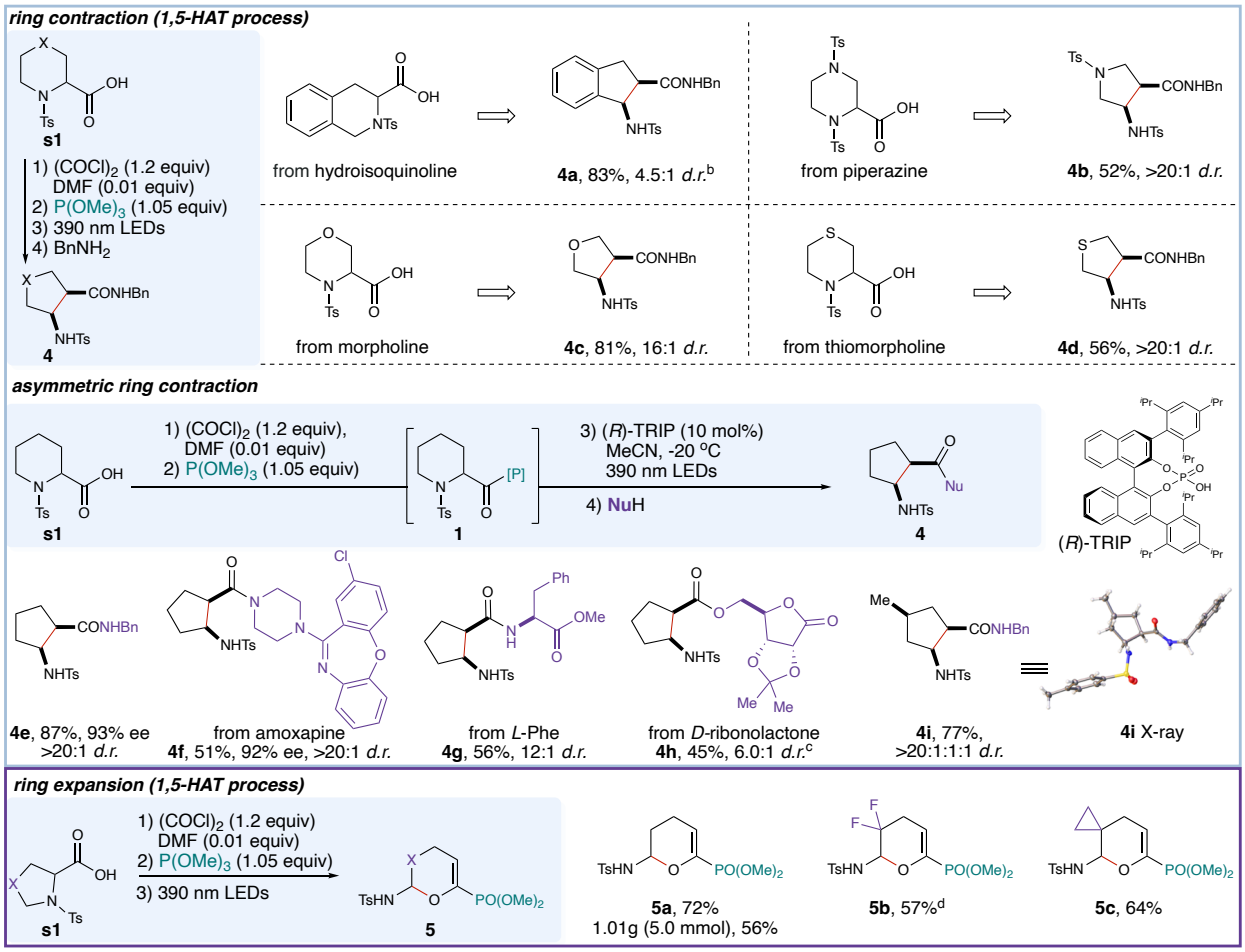

[a]0.20 mmol scale, carboxylic acid as starting material, isolated yield reported, diastereomeric ratios determined by ^{1}H NMR analysis of unpurified reaction mixtures. [b]0.10 equivalent of diphenyl phosphate was added. [c]1.0 equivalent of DBU was added when treated with nucleophile. [d]MeCN was solvent.

Our focus then shifted towards exploring scaffold remodeling of cyclic α-amino acids, guided by the principle that a phosphorus promoter induces a selective 1,5-HAT process (Fig. 4). This process was strategically employed before Mannich or O-nucleophilic addition reactions to achieve ring contraction or expansion. A tetrahydroisoquinoline derivative was successfully transformed into an indene core (**4a**) with a high yield and diastereomeric ratio. Furthermore, piperazine, morpholine, and thiomorpholine derivatives underwent ring contraction to furnish 2,3-*cis*-disubstituted pyrroline (**4b**), tetrahydrofuran (**4c**), and tetrahydrothiophene (**4d**), respectively, with moderate to high yields and excellent diastereoselectivity. Introduction of the chiral phosphoric acid-(*R*)-TRIP catalyst into the reaction system enabled the synthesis of *cis*-2-amino-1-cyclopentanecarboxylic acid derivatives with excellent enantioselectivity (**4e**). We demonstrated the versatility of this phosphorus functional handle by incorporating different functional nucleophiles in the final step, showcasing its utility in the late-stage functionalization of amoxapine (**4f**), *L*-Phe (**4g**), and *D*-ribonolactone (**4h**). Additionally, the transformation of chiral di-substituted piperidine to chiral tri-substituted cyclopentane proceeded with high yield and excellent diastereomeric ratio (**4i**), confirmed by X-ray crystallography to establish its absolute configuration (see the Supporting Information for additional details). Employing α-proline derivatives as starting materials revealed a ring expansion process, furnishing products with good

yields (**5a**). The scalability of this chemistry was validated on a 5.0 mmol scale, resulting in gram-scale product with acceptable yields. Notably, difluoride α-proline (**5b**) and cyclopropane α-proline derivatives (**5c**) were compatible, albeit with moderate yields.

Mechanistic experiments and DFT calculations

The acyl phosphonate intermediate **S1-3d**, obtained through a single-flask transformation, employing a phosphorous promoter, induces a bathochromic shift in the absorbance profile compared with ketone **S1-3a**, ester **S1-3b**, and free carboxylic acid **S1-3c** (Fig. 5a). This shift enables direct photoexcitation under visible light without the need for a sensitizer. Furthermore, employing transient absorption spectroscopy[35] revealed that the acyl phosphonate **S1-3d** significantly increases the half-life of triplet diradicals to 785±4 ns, in contrast to the ketone species **S1-3a**, which only possesses a 195±2 ns half-life[36,37]. To further explore the proposed mechanism, we turned to dispersion-corrected density functional theory (DFT) calculations (see the Supporting Information for additional details).· The first step of the mechanism is presumably the excitation of the acyl phosphonate **1d** under 390 nm wavelength light irradiation followed by ISC to reach the triplet excited state **1d***.[38] To investigate the factors controlling selectivity in the HAT step, we explored different potential HAT pathways emanating from intermediate **1d*** (Fig. 5b). Mulliken's spin density analysis of the optimized **1d*** structure showed significant spin density localized at the oxygen atom, consistent with selective O–H bond formation (vs C–H initiated from the acyl carbon) in the lowest energy HAT step (*vide supra*). Furthermore, consistent with the observed high regioselectivity, the 1,6-HAT takes place through a smaller energy barrier via **TS1** (only 7.0 kcal/mol from **1d***) to form the more thermodynamically stable benzylic 1,5-diradical **A** (11.2 kcal/mol downhill from the excited state intermediate **1d***). In turn, **A** can then undergo irreversible radical-radical C-C coupling to form **2d.** In addition, we explored the alternative 1,4-HAT and 1,5-HAT pathways for the O–H bond formation from **1d*** **(**via **TS2** and **TS3**, respectively). However, the energy barriers were found to be significantly higher (>3 kcal/mol) than the 1,6-HAT process. Notably, although the formation of the **B** radical (1,3-HAT) is thermodynamically favored (7.1 kcal/mol downhill from **1d***), the 1,6-HAT process is both kinetically and thermodynamically favored presumably to a less strain cyclic transition state (**TS1** vs **TS2**; Figure S9) and greater delocalization of the resulting radical intermediate (Table S2). Finally, we also considered the possibility of C–H bond formation initiated from the acyl carbon in **1d*** via **TS1´**, but it was ruled out based on the much higher energy barrier than **TS1** (18.8 vs 7.0 kcal/mol respectively).

Fig. 5. Mechanism study. a) The photophysical properties. (Left) Ultraviolet-visible spectra: 0.1 mM of **S1-3a**, **S1-3b**, **S1-3c**, and **S1-3d** in toluene. (middle) Transient absorption data for **S1-3d** in deaerated toluene excited at 414 nm. (right) Femtosecond time-resolved absorption spectra of **S1-3a** in toluene for 355 nm excitation in the 0.8 ns−300 µs temporal window, **S1-3d** in toluene for 414 nm excitation in the 0.8 ps−300 µs temporal window. b) Proposed mechanism supported by computational studies. Calculated free Gibbs energies [CPCM(toluene) uB3LYP-D3/def2-svp] are given in kcal/mol.

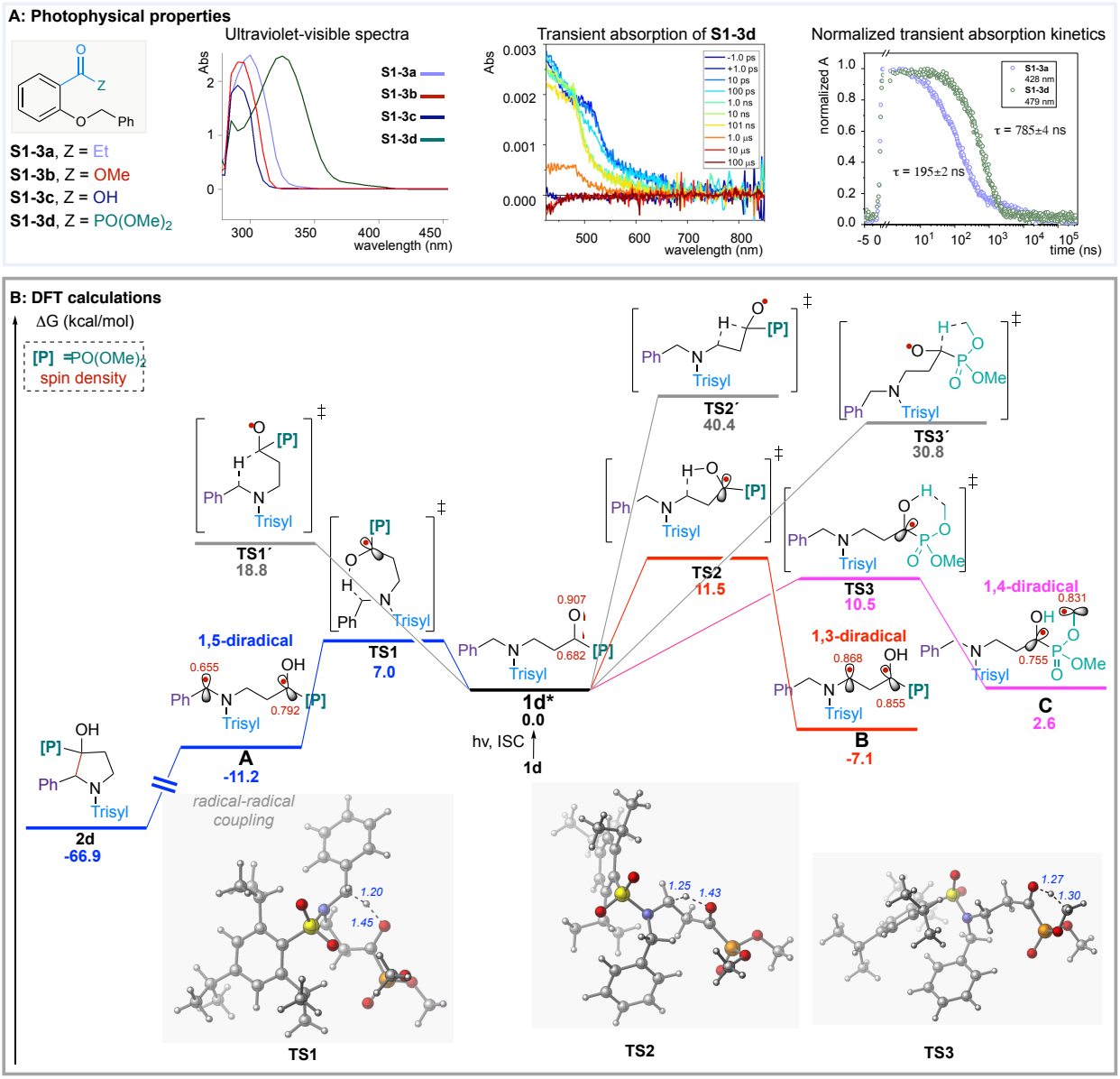

Conclusion

We have devised a comprehensive strategy that leverages triplet carbonyl chemistry, facilitated by a phosphorous promoter, to achieve diverse scaffold remodeling of carboxylic acids. The multifunctionality of the phosphorous promoter also serves as a functional handle for subsequent transformations. A pivotal aspect of our approach involves chromophore activation of carboxylic acids, extending their triplet diradical lifetime and enabling the HAT process. This process has been substantiated through ultrafast spectroscopy experiments and DFT calculations.

References and Notes

1 Prier, C. K., Rankic, D. A. & MacMillan, D. W. C. Visible Light Photoredox Catalysis with Transition Metal Complexes: Applications in Organic Synthesis. *Chem. Rev.* **113**, 5322-5363 (2013).

2 Ravelli, D., Protti, S. & Fagnoni, M. Carbon–Carbon Bond Forming Reactions via Photogenerated Intermediates. *Chem. Rev.* **116**, 9850-9913 (2016).
3 Romero, N. A. & Nicewicz, D. A. Organic Photoredox Catalysis. *Chem. Rev.* **116**, 10075-10166 (2016).
4 Marzo, L., Pagire, S. K., Reiser, O. & König, B. Visible-Light Photocatalysis: Does It Make a Difference in Organic Synthesis? *Angew. Chem. Int. Ed.* **57**, 10034-10072 (2018).
5 Melchiorre, P. Introduction: Photochemical Catalytic Processes. *Chem. Rev.* **122**, 1483-1484 (2022).
6 Norrish, R. G. W. & Bamford, C. H. Photo-decomposition of Aldehydes and Ketones. *Nature* **140**, 195-196 (1937).
7 Yang, N. & Yang, D.-D. H. Photochemical reactions of ketones in solution. *J. Am. Chem. Soc.* **80**, 2913-2914 (1958).
8 Coyle, J. & Carless, H. Selected aspects of photochemistry. I Photochemistry of carbonyl compounds. *Chem. Soc. Rev.* **1**, 465-480 (1972).
9 Burkhard, J. A., Wuitschik, G., Rogers-Evans, M., Müller, K. & Carreira, E. M. Oxetanes as Versatile Elements in Drug Discovery and Synthesis. *Angew. Chem. Int. Ed.* **49**, 9052-9067 (2010).
10 Franceschi, P., Cuadros, S., Goti, G. & Dell'Amico, L. Mechanisms and Synthetic Strategies in Visible Light-Driven [2+2]-Heterocycloadditions. *Angew. Chem. Int. Ed.* **62**, e202217210 (2023).
11 Hoffmann, N. Photochemical reactions as key steps in organic synthesis. *Chem. Rev.* **108**, 1052-1103 (2008).
12 Bach, T. & Hehn, J. P. Photochemical reactions as key steps in natural product synthesis. *Angew. Chem. Int. Ed.* **50**, 1000-1045 (2011).
13 Narayanam, J. M. R. & Stephenson, C. R. J. Visible light photoredox catalysis: applications in organic synthesis. *Chem. Soc. Rev.* **40**, 102-113 (2011).
14 Chen, C. The past, present, and future of the Yang reaction. *Org. Biomol. Chem.* **14**, 8641-8647 (2016).
15 Jurczyk, J., Lux, M. C., Adpressa, D., Kim, S. F., Lam, Y.-h., Yeung, C. S. & Sarpong, R. Photomediated ring contraction of saturated heterocycles. *Science* **373**, 1004-1012 (2021).
16 Cantrell, T. S. Photochemical reactions of benzoic acid. Cycloaddition, hydrogen abstraction, and reverse type II elimination. *J. Am. Chem. Soc.* **95**, 2714-2715 (1973).
17 Brenninger, C., Jolliffe, J. D. & Bach, T. Chromophore Activation of α, β - Unsaturated Carbonyl Compounds and Its Application to Enantioselective Photochemical Reactions. *Angew. Chem. Int. Ed.* **57**, 14338-14349 (2018).
18 Strieth-Kalthoff, F., James, M. J., Teders, M., Pitzer, L. & Glorius, F. Energy transfer catalysis mediated by visible light: principles, applications, directions. *Chem. Soc. Rev.* **47**, 7190-7202 (2018).
19 Kleinmans, R., Pinkert, T., Dutta, S., Paulisch, T. O., Keum, H., Daniliuc, C. G. & Glorius, F. Intermolecular [2π+2σ]-photocycloaddition enabled by triplet energy transfer. *Nature* **605**, 477-482 (2022).
20 Brimioulle, R. & Bach, T. Enantioselective Lewis acid catalysis of intramolecular enone [2+2] photocycloaddition reactions. *Science* **342**, 840-843 (2013).
21 Blum, T. R., Miller, Z. D., Bates, D. M., Guzei, I. A. & Yoon, T. P. Enantioselective photochemistry through Lewis acid–catalyzed triplet energy transfer. *Science* **354**, 1391-1395 (2016).

22 Zuo, Z., Ahneman, D. T., Chu, L., Terrett, J. A., Doyle, A. G. & MacMillan, D. W. C. Merging photoredox with nickel catalysis: Coupling of a-carboxyl sp3-carbons with aryl halides. *Science* **345**, 437-440 (2014).
23 Edwards, J. T., Merchant, R. R., McClymont, K. S., Knouse, K. W., Qin, T., Malins, L. R., Vokits, B., Shaw, S. A., Bao, D.-H., Wei, F.-L., Zhou, T., Eastgate, M. D. & Baran, P. S. Decarboxylative alkenylation. *Nature* **545**, 213-218 (2017).
24 Fawcett, A., Pradeilles, J., Wang, Y., Mutsuga, T., Myers, E. L. & Aggarwal, V. K. Photoinduced decarboxylative borylation of carboxylic acids. *Science* **357**, 283-286 (2017).
25 Ruffoni, A., Hampton, C., Simonetti, M. & Leonori, D. Photoexcited nitroarenes for the oxidative cleavage of alkenes. *Nature* **610**, 81-86 (2022).
26 DiRocco, D. A., Ji, Y., Sherer, E. C., Klapars, A., Reibarkh, M., Dropinski, J., Mathew, R., Maligres, P., Hyde, A. M. & Limanto, J. A multifunctional catalyst that stereoselectively assembles prodrugs. *Science* **356**, 426-430 (2017).
27 Pagire, S. K., Shu, C., Reich, D., Noble, A. & Aggarwal, V. K. Convergent deboronative and decarboxylative phosphonylation enabled by the phosphite radical trap "BecaP". *J. Am. Chem. Soc.* **145**, 18649-18657 (2023).
28 Yin, J., Lin, X., Chai, L., Wang, C.-Y., Zhu, L. & Li, C. Phosphonylation of alkyl radicals. *Chem* **9**, 1945-1954 (2023).
29 Bissonnette, N. B., Bisballe, N., Tran, A. V., Rossi-Ashton, J. A. & MacMillan, D. W. C. Development of a General Organophosphorus Radical Trap: Deoxyphosphonylation of Alcohols. *J. Am. Chem. Soc.* **146**, 7942-7949 (2024).
30 Hu, Y., Stumpfe, D. & Bajorath, J. Recent Advances in Scaffold Hopping. *J. Med. Chem.* **60**, 1238-1246 (2017).
31 Jurczyk, J., Woo, J., Kim, S. F., Dherange, B. D., Sarpong, R. & Levin, M. D. Single-atom logic for heterocycle editing. *Nat. Synth.* **1**, 352-364 (2022).
32 Terauchi, K.-i. & Sakurai, H. Ultraviolet spectral studies in the esters of aroylphosphonic acids. *Bull. Chem. Soc. Jpn.* **42**, 821-823 (1969).
33 Ma, L., Sweet, E. H. & Schultz, P. G. Selective Antibody-Catalyzed Solvolysis of endo-2-Norbornyl Mesylate. *J. Am. Chem. Soc.* **121**, 10227-10228 (1999).
34 Pham, T. Q., Greguric, I., Liu, X., Berghofer, P., Ballantyne, P., Chapman, J., Mattner, F., Dikic, B., Jackson, T., Loc, C. & Katsifis, A. Synthesis and Evaluation of Novel Radioiodinated Benzamides for Malignant Melanoma. *J. Med. Chem.* **50**, 3561-3572 (2007).
35 Aloïse, S., Ruckebusch, C., Blanchet, L., Réhault, J., Buntinx, G. & Huvenne, J.-P. The Benzophenone S1(n, π *) $\rightarrow$ T1(n, π *) States Intersystem Crossing Reinvestigated by Ultrafast Absorption Spectroscopy and Multivariate Curve Resolution. *J. Phys. Chem. A* **112**, 224-231 (2008).
36 Young, R. M., Dyar, S. M., Barnes, J. C., Juríček, M., Stoddart, J. F., Co, D. T. & Wasielewski, M. R. Ultrafast Conformational Dynamics of Electron Transfer in ExBox4+ $\subset$ Perylene. *J. Phys. Chem. A* **117**, 12438-12448 (2013).
37 Wu, Y., Nalluri, S. K. M., Young, R. M., Krzyaniak, M. D., Margulies, E. A., Stoddart, J. F. & Wasielewski, M. R. Charge and Spin Transport in an Organic Molecular Square. *Angew. Chem. Int. Ed.* **54**, 11971-11977 (2015).
38 Peng, Q., Gogoi, A. R., Rentería-Gómez, Á., Gutierrez, O. & Scheidt, K. A. Visible-light-induced coupling of carboxylic acids with alcohols/amines via a phosphorous linchpin strategy. *Chem* **9**, 1983-1993 (2023).

Acknowledgments: The authors thank Dr. Joshua Zhu for assistance with the preparation of this manuscript. The authors thank Saman Shafaie (Northwestern) for assistance with HRMS, Charlotte Stern and Cullen Schull (Northwestern) for assistance with X-ray crystallography respectively.

Funding: We thank the National Institute of General Medical Sciences (R35GM136440) for financial support. This work was supported by the US Department of Energy, Office of Science, Office of Basic Energy Sciences, under award no. DE-FG02-99ER14999 (M.R.W.) O.G. gratefully acknowledges financial support from the National Institutes of Health (R35GM137797). O.G. also acknowledges the Texas A&M University HPRC resources (https://hprc.tamu.edu) for computational resources.

Author contributions: Q.P. and K.A.S. conceived and directed the project. Q.P. and M.H. designed, performed, and analyzed the synthetic chemistry experiments. A.R.-G., P. M., and O. G. designed, performed, and analyzed the computational insight part. R.M.Y. performed and analyzed the transient absorption experiments with samples prepared by Y.Q. Q.P., M.H., A.R.-G., O. G., R.M.Y., and K.A.S. prepared the manuscript. M.R.W., O. G., and K.A.S. acquired funding for the project.

Competing interests: Authors declare that they have no competing interests.

Data and materials availability: All data are available in the main text or the supplementary materials. CCDC 2352355(**2a**) and 2352354 (**4i**) contain the supplemental crystallographic data for this paper. These data can be obtained free of charge via www.ccdc.cam.ac.uk/data_request/cif, or by emailing data_request@ccdc.cam.ac. uk, or by contacting The Cambridge Crystallographic Data Centre, 12 Union Road, Cambridge CB2 1EZ, UK; fax: +44 1223 336033

Supplementary Materials

Materials and Methods

Supplementary Text

Fig. S1 to S9

Tables S1-S4